PCCP

Electrochemical and Ab Initio Investigations to Design New phenothiazine based Organic Redox Polymeric Material for Metal-ion Battery Cathode.

Journal:	*Physical Chemistry Chemical Physics*
Manuscript ID:	CP-ART-03-2015-001495.R2
Article Type:	Paper
Date Submitted by the Author:	06-Aug-2015

Complete List of Authors:	Godet-Bar, Thibault; Univ. Grenoble Alpes/LEPMI, UMR 5279 Leprêtre, Jean-Claude; Univ. Grenoble Alpes/LEPMI, UMR 5279 Le Bacq, Olivier; Univ. Grenoble Alpes/SIMAP, UMR 5266 Sanchez, Jean-Yves; Univ. Grenoble Alpes/LEPMI, UMR 5279 Pasturel, Alain; Univ. Grenoble Alpes/SIMAP, UMR 5266 deronzier, alain; universite de grenoble/CNRS, departement de chimie moleculaire

Cite this: DOI: 10.1039/c0xx00000x

www.rsc.org/xxxxxx

ARTICLE TYPE

Electrochemical and *Ab Initio* Investigations to Design New phenothiazine based Organic Redox Polymeric Material for Metal-ion Battery Cathode.

Dr. T. Godet-Bar,*[a] Prof. J.-C. Leprêtre,[a] Dr. O. Le Bacq[b], Prof. J.-Y. Sanchez,[a] Dir. of Res. A. Deronzier,[b] and Prof. A. Pasturel[c]

Received (in XXX, XXX) Xth XXXXXXXXX 20XX, Accepted Xth XXXXXXXXX 20XX
DOI: 10.1039/b000000x

Different *N*-substituted phenothiazines have been synthesized and their electrochemical behavior has been investigated in CH_3CN in order to design the best polyphenothiazine based cathodic material candidate for lithium batteries. These compounds exhibit two successive reversible one-electron oxidation processes. *Ab initio* calculations demonstrate that the potential of the first one is a result of both the hybridization effects between the substituent and the phenothiazine unit as well as the change of conformation adopted by the phenothiazine heterocycle along with the oxidation process. More specifically, we show that an asymmetric molecular orbital spreading throughout an external cycle of the phenothiazine unit and the alkyl fragment is formed only if the alkyl fragment is long enough (from methyl moiety and after) and is at the origin of the bent conformation for *N*-substituted phenothiazines during oxidation. Electrochemical investigations supported by *ab initio* calculations allow selecting a phenothiazinyl unit which is then polymerized by a Suzuki coupling strategy to avoid the common solubilization issue in carbonate-based liquid electrolyte of lithium cells. The first electrochemical measurements performed show that phenothiazine derivatives pave the way for a promising family of redox polymers intended to be used as organic positives for lithium batteries.

Keywords: phenothiazines, organic cathode materials, *ab initio* calculation, metal-ion battery

1. Introduction

In the scope of improving the lithium battery safety, cost, environmental impact and performances, many strategies are currently developed. The safety concerns mainly the O_2 release due to a progressive degradation of layered and spinel cathodic oxide materials[1,2]. The development of olivine cathode materials ($LiMPO_4$, M = Mn, Fe, Co, or Ni[3]) gets rid of that phenomenon thanks to strong P-O interactions preventing oxygen leaks. As long as electrolytes are unstable at high potentials, $LiFePO_4$ remains the best inorganic cathode material nowadays with no safety and toxicity issues, with quite good specific discharge capacities and high cyclability. Nevertheless, this material exhibits relative low redox potential (3.45 V/Li/Li^+) and suffers from low electronic conductivity which implies adapted nanoparticles synthesis (*i.e.* carbon coating) and thus non negligible additional costs[4].

Concerning performances, efforts are devoted both to high potential material elaboration and electrolyte stability upgrade. Beside electrolyte based researches involving additives[5,6], many studies are dedicated to new cathodic materials[7]. In this context, apart from regular works involving transition metal species, the organic materials alternative constitutes a breakthrough in cathode materials elaboration due to low costs and toxicity, a wide choice of organic families that can reach high potentials and capacities. Moreover, their versatility towards cation due to their higher flexibility than rigid inorganic hosts allow them to be used in alkaline (sodium[8]) and alkaline earth metal batteries.

The main drawback of these compounds remains the progressive dissolution throughout their cycling. The two main strategies involved to overcome this issue consist on either the use of an insoluble redox monomer as described for quinoïd molecules bearing charged anion-based salts[9,10] or polymers exhibiting electrochemical properties. Some of them are themselves redox-active like polyaniline[11], polypyrrole[8], or polyanthraquinones[12]; and others are used as hosts for incorporated redox active molecules. For the latter category, one can emphasize that since few years Nishide *et al.* pioneered the development of organic radical battery using 2,2,6,6-tetramethylpiperidine-1-oxyl (TEMPO) derivative grafted onto polymeric material[13-15].

Battery tests involving these materials displayed relative high performance regarding mass capacity and durability. These promising materials tend to compete with regular inorganic material but they need to exhibit higher anodic potential value while maintaining a good mass capacity and a good cyclability.

In this work, we chose to synthesize and study a new kind of organic polymeric cathode based on *N*-substituted phenothiazine,

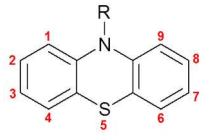

Scheme 1 Phenothiazine molecule

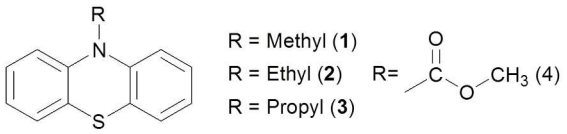

Scheme 2 Structure of the studied modified phenothiazine

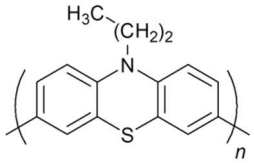

Scheme 3 Structure of **Poly3**

(**Scheme 1**) a type of compound commonly used in pharmacopoeia as anthelmintic[16], antihistamine and antimicrobial[17], psychotherapeutic with chloropromazine[18] or in chemotherapy[19].

The redox properties of those molecules have been used as redox shuttle[20-22] in $LiFePO_4$/graphite and in the field of electrochromic or NADH detection[23], but rarely as redox material for battery. Only few battery tests of polyphenothiazine have been performed showing poor performances[24] although phenothiazines (**PT**) especially *N*-substituted ones are known since the beginning of the sixties for its reversible first one-electron oxidation at 3.9[25-27] V/Li/Li^+. In addition, as recalled above since the development of its use as medical drugs shows that **PT** can be easily chemically modified allowing to advantageously modulate its oxidation potential whereas a two successive oxidation processes can be investigated.

Here, we propose a new organic material involving polymeric **PT**. Thanks to adapted chemical modification, oxidation potential is expected to be modulated. In a first step, we analyzed mainly the influence of the *N*-chemical modification towards anodic behavior of the studied compounds (**Scheme 2**) using electrochemical investigation associated with *ab initio* calculations.

From an experimental point of view, we focused on the best redox reversibility and on the higher oxidation potential in view to determine the best target to be involved in polymeric **PT**. These criteria have been chosen in view i) to reach high powerful system while respecting the electrolyte stability ii) to reach the higher mass capacity, knowing that the weaker is its unity molecular mass undergoing the electron transfer, the higher its performance should be.

The experimental analyses of **PT** derivatives are supplemented by a theoretical investigation through *ab initio* calculations aiming at providing a theoretical explanation for the change in electrochemical properties and kinetics of charge transfer.

Finally, after this preliminary electrochemical investigation, a convenient candidate is selected (*vide infra*) to be tested as polymeric material. The polymerization procedure has been performed according to an adapted Suzuki coupling method[28-30] and has led to an alkyl derivative, the poly-*N*-propylphenothiazine (**Poly3**) (**Scheme 3**). We report also here first results about the electrochemical behavior of **Poly3** in CME and in a preliminary lithium cell test.

2. Methodologies

Synthesis: The purity of the synthesized compounds has been checked by ^{1}H NMR, ^{13}C NMR, IR and elemental analysis. NMR has been measured using a 400 MHz Brücker and Fourier transform infrared (FT-IR) spectra were recorded on a Brücker Vertex 70v FT-IR spectrometer using KBr pellets. The elemental analyses have been performed in a CNRS certified company "the Service Central d'Analyse of the CNRS at Solaize (France)".

Alkyl derivatives **1**, **2** and **3** have been synthesized according to the same experimental conditions[31]. To a **PT** (5.0 g, 25 mmol, Acros, 99 %) dissolved in freshly distilled DMSO (60 mL) solution, 2.5 molar equiv of potassium hydroxide (3.6 g, 64 mmol) were added. The solution was stirred at room temperature for 30 min prior to the addition of 1.1 molar equiv of 1-bromoalkyl (27 mmol, Sigma, 99 %). After 24 hours refluxing, the solution was cooled to room temperature. The solution was poured into water (300 mL); the precipitate was filtered and extracted by dichloromethane (4x10 mL). The collected organic layers were dried over sodium sulfate, filtered and concentrated under reduced pressure. After purification over a silica gel column (eluent = pentane), the product was obtained as a white (**1**), and light yellow (**2** and **3**) powder with 86 to 95 % yield.

***N*-methylphenothiazine (1)**. Found: C, 72.90; H, 5.25; N, 6.50; S, 14.95. Calc. for $C_{13}H_{11}NS$ (213.30 g.mol^{-1}): C, 73.20; H, 5.20; N, 6.57; S, 15.03%. ν_{max}/cm^{-1} 3053 (CC), 1592 (CC), 1569 (CC), 1456 (CH), 1282 (CN), 758 (CH). δ_H (400 MHz; $(CD_3)_2CO$; 300 K) 3.33 (s, 3H, CH_3), 6.90 (dd, ^3J = 8.2 Hz, ^4J = 1.0 Hz, 2H; Ar H), 6.94 (dt, ^3J = 7.5 Hz, ^4J = 1.2 Hz, 2H; Ar H), 7.13 (dd, ^3J = 7.6 Hz, ^4J = 1.5 Hz, 2H; Ar H), 7.20 (dt, ^3J = 7.4 Hz, ^4J = 1.5 Hz and 0.7 Hz, 2H; Ar H). δ_C (100 MHz; CD_3CN; 300 K) 35.73 (CH_3), 115.34 (CH), 123.36 (CH), 123.67 (C_{quat}), 127.71 (CH), 128.56 (CH), 146.65 (C_{quat}). TLC: R_f = 0.63 (eluent = 3:5 dichloromethane:hexane).

***N*-ethylphenothiazine (2)**. Found: C, 73.95; H, 5.70; N, 6.15; S, 14.20. Calc. for $C_{14}H_{13}NS$ (227.32 g.mol^{-1}): C, 73.97; H, 5.76; N, 6.16; S, 14.11%. ν_{max}/cm^{-1} 2971 (CH), 1591 (CC), 1569 (CC), 1459 (CH), 1281 (CN), 756 (CH). δ_H (400 MHz; CD_3CN; 300 K) 1.37 (t, ^3J = 6.9 Hz, 3H; CH_3), 3.98 (q, ^3J = 6.9 Hz, 2H; CH_2), 6.92 (dt, ^3J = 7.4 Hz, ^4J = 1.3 Hz, 2H; Ar H), 7.00 (dd, ^3J = 8.2 Hz, ^4J = 1.3 Hz, 2H; Ar H), 7.12 (dd, ^3J = 7.7 Hz, ^4J = 1.5 Hz, 2H; Ar H), 7.18 (dt, ^3J = 7.4 Hz, ^4J = 1.5 Hz, 2H; Ar H). δ_C (100 MHz; $(CD_3)_2CO$; 300 K) 13.4 (CH_3), 42.3 (CH_2), 116.4 (CH), 123.3 (CH), 125.1 (C_{quat}), 128.0 (CH), 128.4 (CH), 146.1 (C_{quat}). TLC: R_f = 0.41 (eluent = hexane).

***N*-propylphenothiazine (3)**. Found: C, 73.90; H, 6.05; N, 5.75, S, 13.55. Calc. for $C_{15}H_{15}NS$ (241.35 g.mol^{-1}): C, 74.65; H, 6.26; N, 5.80; S, 13.29%. ν_{max}/cm^{-1} 3000 (CC), 1593 (CC), 1570 (CC), 1461 (CH), 1337 (CN), 752 (CH). δ_H (400 MHz; $(CD_3)_2SO$; 300 K) 0.92 (t, ^3J = 7.2 Hz, 3H; CH_3), 1.68 (tq, ^3J = 6.9 Hz and 7.2 Hz, 2H; CH_2), 3.81 (t, ^3J = 6.9 Hz, 2H; CH_2), 6.92 (dt, ^3J = 7.4 Hz, 2H; Ar H) ; 6.99 (dd, ^3J = 7.9 Hz, 2H; Ar H), 7.13 (dd, ^3J = 7.4 Hz, 2H; Ar H), 7.18 (dt, ^3J = 7.9 Hz, 2H; Ar H). δ_C (100

MHz; $(CD_3)_2SO$; 300 K) 11.0 (CH_3), 19.5 (CH_2), 48.1 (CH_2), 115.8 (CH), 122.3 (CH), 123.6 (C_{quat}), 127.0 (CH), 127.5 (CH), 144.7 (C_{quat}). TLC: R_f = 0.44 (eluent = hexane).

***N*-methylcarboxylate-phenothiazine (4)**. **4** has been obtained by reaction of phenothiazine-10-carbonyl chloride (1.0 g, 3.8 mmol, Acros, 98 %) in methanol[32] (100 mL) at reflux for 12 hours. After cooling, methanol is removed under reduced pressure and aqueous saturated $NaHCO_3$ (30 mL) were added, the aqueous phase was extracted with dichloromethane (3x30 mL). The purification over silica gel of combined organic extracts (eluent = 3:10 dichloromethane:pentane) provided a white powder.

***N*-methylcarboxylatephenothiazine (4)** (0.61 g, 62 %). Found: C, 65.75; H, 4.25; N, 5.45. Calc. for $C_{14}H_{11}NO_2S$ (257.31 g.mol^{-1}): C, 65.40; H, 4.31; N, 5.44%. ν_{max}/cm^{-1} 3067 (CC), 1712 (CO), 1589 (CC), 1566 (CC), 1465 (CH), 1263 (CN), 759 (CH). δ_H (400 MHz; CD_3CN; 300 K) 3.73 (s, 3H, CH_3), 7.22 (dt, ^3J = 7.6 Hz, ^4J = 1.3 Hz, 2H; Ar H), 7.33 (dt, ^3J = 7.7 Hz, ^4J = 1.4 Hz and 0.5 Hz, 2H; Ar H), 7.41 (dd, ^3J = 7.8 Hz, ^4J = 1.5 Hz, 2H; Ar H), 7.57 (dd, ^3J = 8.1 Hz, ^4J = 1.3 Hz, 2H; Ar H). δ_C (100 MHz; CD_3CN; 300 K) 53.94 (CH_3), 127.50 (CH), 127.98 (CH), 128.07 (CH), 128.35 (CH), 132.81 (C_{quat}), 139.33 (C_{quat}), 154.67 (C_{quat}). TLC: R_f = 0.50 (eluent = 1:1 dichloromethane:hexane).

3,7-dibromo-*N*-propylphenothiazine (5). **5** has been synthesized following a procedure adapted from M. Sailer *et al.*[30] To a solution of **3** (5.5 g, 22.8 mmol) in freshly distilled acetic acid solution (10 mL), one molar equivalent of bromine (1.17 mL, 22.8 mmol, Aldrich, reagent grade) was added dropwise. The mixture was stirred for one hour before another portion of bromine (1.17 mL, 22.8 mmol) was added drop wise. After 18 hours of stirring and a complete conversion of the starting material (checked by TLC using acetone:hexane 1:20 as eluent), satured aqueous sulfite sodium (20 mL) and diethyl ether (20 mL) were added to the mixture, which was then stirred for 2 hours. The aqueous layer was extracted with diethyl ether (3x15 mL) and the collected organic layers were concentrated in vacuum. After purification over a silica gel column using acetone:hexane 1:100 as eluent, a slightly yellow powder was obtained.

3,7-dibromo-*N*-propylphenothiazine (5) (8.65 g, 95 %). Found: C, 45.20; H, 3.20; N, 3.70; S, 7.50; Br, 39.80. Calc. for $C_{15}H_{13}Br_2NS$ (399.14 g.mol^{-1}): C, 45.14; H, 3.28; N, 3.51; S, 8.03; Br, 40.04%. ν_{max}/cm^{-1} 2976 (CH), 1585 (CC), 1461 (CH), 1248 (CN), 878 (CH), 807 (CH), 739 (CH), 648 (CBr). δ_H (300 MHz; $CDCl_3$; 300 K) 1.00 (t, ^3J = 7.4 Hz, 3H; CH_3), 1.70 (hex, ^3J = 7.2 Hz, 2H; CH_2), 3.69 (t, ^3J = 6.7 Hz, 2H; CH_2), 6.63 (d, ^3J = 8.4 Hz, 2H; Ar H), 7.18 (d, ^4J = 2.0 Hz, 2H; Ar H), 7.21 (dd, ^3J = 8.4 Hz, ^4J = 2.0 Hz, 2H; Ar H). δ_C (100 MHz; $CDCl_3$; 300 K) 11.09 (CH_3), 19.70 (CH_2), 48.99 (CH_2), 114.46 (C-Br), 116.39 (CH), 126.08 (C_{quat}), 129.31 (CH), 129.81 (CH), 143.69 (C_{quat}). TLC: R_f = 0.59 (eluent = 1:19 acetone:hexane).

3,7-bis(4,4,5,5-tetramethyl-1,3,2-dioxaborolan-2-yl)-*N*-propylphenothiazine (6) (0.389 mg, 63 %). This product has been synthesized following the procedure of J. Choi *et al.*[28] To a **5** (500 mg, 1.25 mmol) in 10 mL freshly distilled and argon flushed and stirred THF solution at -80°C, 2.5 molar equivalent of *N*-BuLi (1.6 M in hexane solution, Aldrich) (1.25 mL, 3.125 mmol) were added dropwise. The solution was kept at -80°C over 2 hours before the addition of 2.5 molar equivalents of 2-isopropoxy-4,4,5,5-tetramethyl-1,3,2-dioxaborolane (0.65 mL, 3.125 mmol, Aldrich, 98%). The solution was then kept at -80°C over 5 hours before it was allowed to reach R.T. The stirring is then pursued for 18 hours. The THF is evaporated in vacuum and 100 mL of distilled water were added. The aqueous layer was extracted with 4x25 mL of dichloromethane and the collected organic layers were concentrated *in vacuum*. The product was then recristallized from acetonitrile (1 g for 30 mL) and provided a light yellow powder.

3,7-bis(4,4,5,5-tetramethyl-1,3,2-dioxaborolan-2-yl)-*N*-propylphenothiazine (6) (0.389 mg, 63 %). Found: C, 65.09; H, 7.49; N, 2.72. Calc. for $C_{27}H_{37}B_2NO_4S$ (493.27 g.mol^{-1}): C, 65.74; H, 7.56; N, 2.84. ν_{max}/cm^{-1} 3005 (CC), 1581 (CC), 1470 (CH), 1352 (BO), 1263 (CN), 1144 (CO), 1101 (CO), 856 (CH), 673 (CH). δ_H (400 MHz; $(CD_3)_2SO$; 300 K) 0.92 (t, ^3J = 7.3 Hz, 3H; CH_3), 1.27 (s, 24H; CH_3), 1.68 (dd, ^3J = 7.0 and 7.3 Hz, 2H; CH_2), 3.86 (t, ^3J = 7.0 Hz, 2H; CH_2), 7.01 (d, ^3J = 8,3 Hz, 2H; Ar H), 7,31 (d, ^4J = 1,4 Hz, 2H; Ar H), 7,47 (dd, ^3J = 8,3 Hz, ^4J = 1,4 Hz, 2H, Ar H).

The polymerization was performed using microwave irradiation in a CEM Discover S-class apparatus following a procedure based on multiple works[28-30].

Poly-*N*-propylphenothiazine (Poly3a). To 2.7 mL of dimethoxyethane (DME) and 1.3 mL of water flushed with argon for 30 minutes, 1 molar equivalent of **5** (100 mg, 2.25.10^{-4} mol), 1 molar equivalent of **6** (123.5 mg, 2.25.10^{-4} mol), 5 molar equivalent of carbonate potassium (173 mg, 1,25 mmol) and 4 % molar of [1,1-Bis(diphenylphosphino)ferrocene]-dichloropalladium(II) ($PdCl_2$dppf) (7.5 mg, 1.03.10^{-5} mol, Aldrich) were added. The mixture was submitted to microwave treatment (150 Watts, 19 bars, 190°C) during 15 min leading to a black solution. Then, 10 mg of **6** is added to the mixture which is submitted again to microwaves treatment under the same conditions during 5 minutes.

After cooling, polymer was precipitated by addition of 300 mL of water. The crude material was carefully milled in an agate mortar and washed with warm water, acetonitrile, methanol and diethyl ether. The black powder was washed on methanol soxhlet for 3 days and was finally washed with warm dimethylsulfoxide, methanol and dichloromethane (DCM).

This led to a brown powder insoluble in numerous solvents preventing its NMR and GPC investigations.

Poly-*N*-propylphenothiazine (Poly3a) (20 mg, 17 %). Found: C, 71.27; H, 5.31; N, 5.26. Calc. for $(C_{15}H_{15}NS)_n$ (239.34 g.mol^{-1})$_n$: C, 75.28; H, 5.47; N, 5.85. ν_{max}/cm^{-1} 2960 (CH), 1605 (CC), 1457 (CH), 1227 (CN), 872 (CH), 804 (CH), 734 (CH). SEM-EDX confirmed presence of ~1 % of Pd and ~1 % of Br.

Poly-*N*-propylphenothiazine (Poly3b). The same procedure as **Poly3a**'s has been followed except that in this case, 1 % molar equivalent of $PdCl_2$dppf was used to catalyze the reaction (1.9 mg, 2.58.10^{-6} mol).

After the addition of **6** followed by microwaves treatment and cooling, the polymer was precipitated by addition of 300 mL of water. The crude material was carefully milled in an agate mortar and washed with warm water, acetonitrile, methanol and diethyl ether. To the black powder was added 10 mL of DCM, the solution was filtrated and carefully washed with warm DCM. The organic layer was concentrated, passed through a celite plug, concentrated under vacuum and was washed on methanol soxhlet

Cite this: DOI: 10.1039/c0xx00000x

www.rsc.org/xxxxxx

ARTICLE TYPE

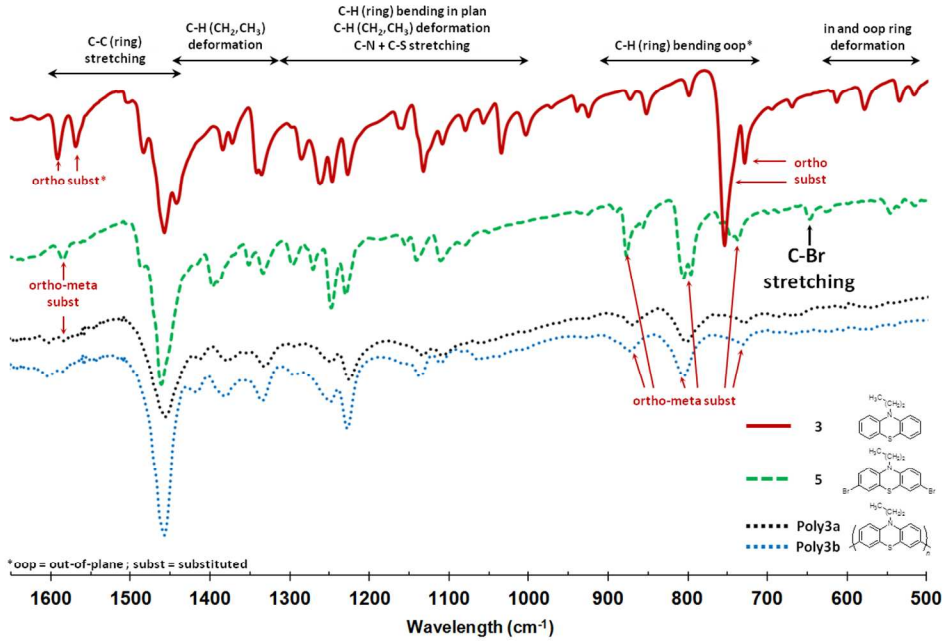

Fig. 1 FTIR of **3** (red full line), of **5** (green dashed line), of **Poly3a** (black dotted line) and of **Poly3b** (blue dotted line) recorded between 500 and 1650 cm^{-1}

for 3 days to yield a black powder. Its low solubility in organic solvents prevented its ^{13}C NMR and GPC investigations.

Poly-*N*-propylphenothiazine (Poly3b) (58 mg, 48 %). Found: C, 70.75; H, 5.21; N, 4.97. Calc. for $(C_{15}H_{15}NS)_n$ (239.34 $g.mol^{-1}$)$_n$: C, 75.28; H, 5.47; N, 5.85. ν_{max}/cm^{-1} 2962 (CH), 1606 (CC), 1458 (CH), 1228 (CN), 874 (CH), 807 (CH), 737 (CH). δ_H (400 MHz; $CDCl_3$; 300 K) 0.89 (m, 3H; CH_3), 1.85 (m, 2H; CH_2), 3.83 (m, 2H; CH_2), 6.87 (m, 2H; Ar H), 7.30 (m, 4H; Ar H).

Electrochemistry: All electrochemical measurements were performed under an argon atmosphere in a dry-glove box at room temperature. Acetonitrile (CH_3CN, Rathburn, HPLC grade), tetra-*N*-butyl-ammonium perchlorate (TBAP, Fluka), were used as received and stored under an argon atmosphere. In these experimental conditions the amount of H_2O in electrolyte is less than 10 ppm. Cyclic voltammetry experiments were performed using a Biologic SP-300 potentiostat/galvanostat equipped with a standard three electrodes electrochemical cell. Potentials were referred to an Ag/0.01 $mol.L^{-1}$ $AgNO_3$ reference electrode in CH_3CN + 0.1 $mol.L^{-1}$ TBAP. The potentials were corrected to the internal standard of the ferrocene in CH_3CN, $E_{1/2}^{0/+1}$ = 0.087 V /Ag/$AgNO_3$[33]) and then converted to Li/Li^+ scale by adding 3.588 V in order to refer the redox properties of our materials to the alkaline mostly used as negative electrode in the metal-ion battery field. The working electrodes, polished with 2 µm diamond paste (MecaprexPresi), were a platinum disk (5 mm in diameter) or a vitreous carbon disk (3 mm in diameter) for cyclic voltammetry. $E_{p,a}$ and $E_{p,c}$ correspond to the anodic peak and the cathodic peak potentials respectively (**Equation 1**). The background current does not exceed 8 µA at 100 $mV.s^{-1}$ in the potential range explored with Pt 2 mm electrode.

$$E_{1/2} = \frac{E_{p,a}+E_{p,c}}{2}; \Delta E_p = E_{p,a} - E_{p,c} \quad (1)$$

The cavity microelectrode, provided by origin consisted of a platinum microelectrode (diameter 100 µm) sealed in glass. A microcavity was obtained by a controlled dissolution of the Pt-wire in a concentrated hot (80 °C) solution of *aqua regia* for 20 min. The deepness of the cavity of 20 µm was measured by an optical microscope. Current peaks $i_{p,a}$ and $i_{p,c}$ and potential peaks $E_{p,a}$ and $E_{p,c}$ were measured at the oxidation peak and at the reduction peak taking into account the capacitive current. Due to the extended redox processes of the polymer and the close redox systems, we were not able to obtain an accurate lecture of the capacitive current in the cyclic voltammograms performed, thus, coulombic and capacitive charges were not calculated.

Cell tests have been carried out in a 9 mm diameter Swagelok system. A slurry for the positive electrode was prepared by mixing **Poly3a**, carbon C-65 (Super P®, Timcal), vapor-grown carbon fibers (VGCF®, Showa Denko), and PVdF 6020 (Solef®, Solvay) in a weight ratio of 65:20:5:10 with *N*-methylpyrrolidone (10% w). The prepared slurry was then dropcoated on an Inox® 8 mm disc. The electrolyte used was LP-30 (EC-DMC 1:1 %w + $LiPF_6$ 1 M, Powerlyte UBE Europe GmbH), Karl Fisher titration permitted an estimation of 18 ppm of water content. A lithium

disc (Rockwood Lithium) was used as negative electrode. The

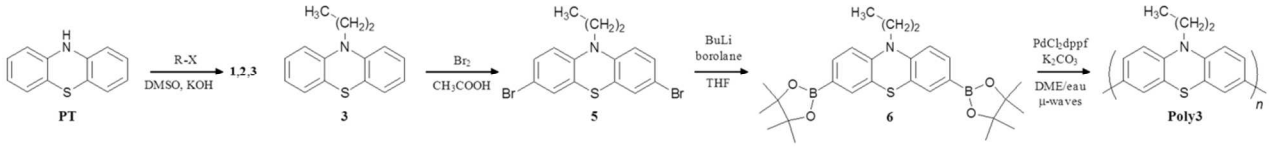

Scheme 4 Synthesis of the phenothiazine based materials

Swagelok cell was assembled in an argon-filled glove box containing < 10 ppm of oxygen and < 3 ppm of water. The positive electrode was loaded with 3.12 mg.cm^{-2} of slurry formulation, its thickness was of 76 ± 2 µm.

Galvanostatic and cyclic voltammetry measurements were carried out between 3 and 4 V /Li/Li^{+} at 25 °C using a Solartron 147 Battery test unit.

Computational method: *Ab initio* calculations using density functional theory have been performed in order to explain the trends observed. All the DFT calculations are done with the BIGDFT electronic structure code[34] which uses a systematic wavelet basis. This DFT method is based on Kohn-Sham (KS) orbitals instead of the Hartree-Fock (HF) molecular orbitals (MO). However, it is today well established that the KS orbitals lead to similar symmetry, shape and energies than those obtained by the HF method, allowing a proper interpretation of the molecular orbitals[35,36]. Moreover the KS orbitals have been widely used to study the electronic structure of molecular systems[37]. The pseudopotentials used in the present study are the ones developed by Gödecker et al.[38] within the Local-Density Approximation (LDA) and initially developed within the framework of the Abinit code. This latter approximation for the exchange and correlation potential were found convenient to recover good agreement between the calculated and experimental geometric parameters (interatomic distances) of **PT**. We considered the basis converged when an accuracy of 0.5 meV/atom was reached for the total energy and 1 meV/Å for the forces. This corresponds to a uniform wavelet grid with a spacing of 0.35 bohr with an extent of 5.0 bohrs for the coarse grid and 8.0 bohrs for the fine grid. Thus, we determined the atomic positions of the four molecules considered in both the neutral and oxidized states optimized at 0 Kelvin and data defining the conformation of their respective ground state.

3. Results & Discussion

3.1. Synthesis

The syntheses of the functionalized **PT** (Scheme 2) have been performed following procedures from the literature[30-32]. The polyphenothiazine **Poly3** (Scheme 3) have been synthesized using adapted procedures[28,29,39].

PT is commercially available. For nitrogen functionnalized phenothiazine (**1**-**4**), the starting material was mainly **PT** except for the ester derivative **4** where the commercially available phenothiazine-*N*-carbonyl chloride has been used. In all cases, the one step reaction leads to pure compounds in high yield. FT-IR spectra (**Figure 1**) of the propyl derivative (**3**) shows typical phenothiazine vibration bands with ortho disubstituted aromatic rings[40,41] *i.e.* the two C-C ring stretching bands at 1593 (medium) and 1570 (medium) cm^{-1} and the two C-H ring bending out-of-plane bands at 752 (strong) and 730 (weak) cm^{-1}. Concerning bromo derivative (**5**) (**Scheme 4**), due to the strong oxidizing character of the experimental conditions (Br_2), sulfoxides side products are often produced[42,43]. However, using a reducing agent in the second step (*i.e.* sodium sulfite), the expected products have been obtained in good yields. Concerning polymeric material (Scheme 3), phenothiazine **3** has been selected (*vide infra*).

The pinacol ester propyl derivative (**6**) (Scheme 4) was synthesized by borylation of **5** in THF in presence of BuLi and isopropoxyborolane[28] with a 63 % yield (80 % borylation yield per bromide).

After bromination (**5**) and borylation (**6**), the Suzuki coupling reaction has been carried out leading to the homopolymer **Poly3**. Usual amounts of catalyst (4 % molar equivalent of $PdCl_2$dppf) lead to 17 % of insoluble polymer **Poly3a** whereas using lower amounts (1 %) only 4 % **Poly3a** are obtained. For the latter, the main product **Poly3b** is soluble in DCM. One can suggest that lower amounts of catalyst leads to polymers with shorter chains, and thus higher solubility in organic solvents. As a result, 1H NMR of **Poly3b** can be performed in $CDCl_3$. This analysis confirms the polymer structure as judged by the observation of an ortho-meta substituted *N*-propylphenothiazine skeleton, whereas some traces of terminal pinacol ester are detected (δ = 1.32 ppm) with a phenothiazine/pinacol ester molar ratio of about 6/2.

FT-IR spectra (Figure 1) of homopolymers **Poly3a** and **Poly3b** are similar, which attests that they share the same structure. Monomer (**5**) and homopolymers show close vibration signatures with typical ortho-meta trisubstituted aromatic rings[40,41] *e.g.* 3 vibration band groups at the vicinity of 870, 800 and 730 cm^{-1} while C-Br stretching vibration band observable for the brominated derivative (**5**) at 648 cm^{-1} is no longer present in the polymer, which is in good agreement with the residual bromide amount (1 %) measured, by SEM-EDX, in the **Poly3a**.

For **Poly3a**, even if the accurate attribution of terminal pinacol ester (B-O vibration at 1350 cm^{-1} and C-O vibration at 1140 and 1100 cm^{-1}) is not easy due to the presence of other polyphenothiazine skeleton vibrations, one cannot exclude the presence of such terminal function.

Table 1 $E_{1/2}$ and k° for phenothiazine derivativesnin CH_3CN + TBAP 0.1 M on a platinum electrode (diam. 2 mm), $E_{1/2}$ determined at 50 mV s^{-1}

	$E^1_{1/2}$ /Li/Li$^+$, (ΔE_p)	$E^2_{1/2}$ /Li/Li$^+$, (ΔE_p)	k^0 /10^{-3} cm s^{-1}
PT	3.89 V, (100 mV)	4.43 V, (160 mV)	4.44 (± 0.12)
1	4.00 V, (95 mV)	4.65 V, (95 mV)	5.56 (± 0.10)
2	3.97 V, (95 mV)	4.63 V, (95 mV)	5.74 (± 0.06)
3	3.97 V, (90 mV)	4.63 V, (90 mV)	5.87 (± 0.07)

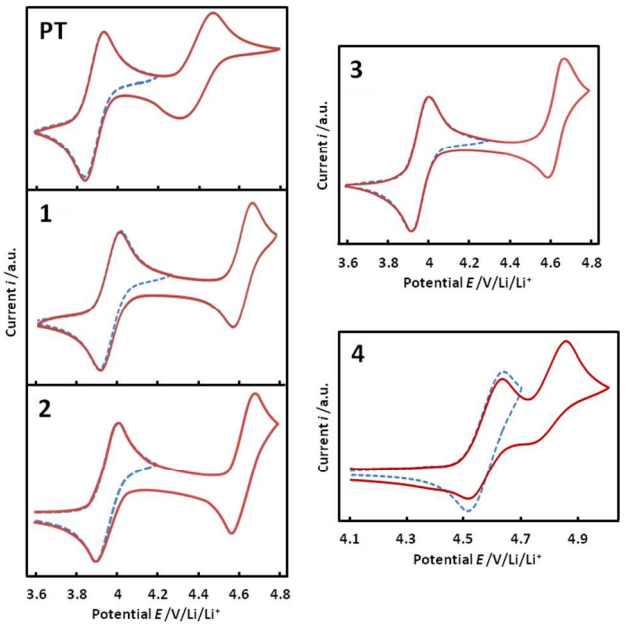

Fig. 2 Cycling voltammograms recorded at 50 mV.s^{-1} showing (blue dashed line) the first redox system and (red full line) the two redox systems of compounds **PT**, **1**, **2**, **3** and **4** at ~5.10^{-3} M in CH_3CN + TBAP 0.1 M medium

Regarding elemental analyses, **Poly3b** displayed a %C and a %N in good agreement with a polyphenothiazine endcapped with boronic function with a molar ratio phenothiazine/pinacol ester in accordance with ^{1}H NMR analysis. Based on %C and %N comparison, **Poly3a** exhibits as expected a higher phenothiazine content.

Despite the presence of additive side products, the purity of these materials is considered acceptable for further electrochemical analyses. Obviously, we chose to investigate the one with the lower solubility in organic solvents *i.e.* the **Poly3a** in order to avoid dissolution in cell test conditions (liquid carbonates based electrolyte).

3.2. Electrochemistry of phenothiazine based monomers

3.2.1. Experimental investigation

This electrochemical investigation is focused on the selection of the redox target exhibiting a high electrochemical reversibility of its oxidation and a high $E_{1/2}$ value. In addition, this value has to be consistent with the electrolyte electrochemical stability. The usual carbonate based electrolyte being considered as reference for lithium-ion batteries, $E_{1/2}$ values have to be lower than 4.5 V/Li/Li$^+$ (*i.e.* 1.5 V/SHE) since higher oxidative character could lead to the progressive electrolyte degradation[44].

Moreover, although phenothiazine derivatives have been electrochemically studied in numerous conditions (aqueous medium in the presence of acidic species[43] in SO_2 medium[45], in organic electrolytes[27,46]), we chose to perform this analysis in more adapted conditions *e.g.* anhydrous CH_3CN (H_2O < 10 ppm) in the presence of TBAP 0.1 M.

The CV exhibits, for **PT**, a first one electron oxidation at $E_{1/2}$ = 3.89 V/Li/Li$^+$ (**Figure 2**). Upon different scan rates, i) only slight variation of $E^1_{p,a}$ and $E^1_{p,c}$ is observed, ii) $i_{p,a}/i_{p,c}$ stays close to the unity, iii) ΔE_p values change around 100 ± 10 mV, iv) $i_{p,a}$ and $i_{p,c}$ are proportional to the square root of the scan rate. These parameters are consistent with a fast and quasi-reversible process[47]. On the other hand, the second one-electron transfer appears slower and less reversible with a ΔE_p increasing along with the scan rate decrease (**Table 1**).

This behavior is due to the strong acidic character of the two one-electron oxidized form of **PT** which can undergo a deprotonation step[27].

One can notice that the side reaction leading to sulfoxide derivatives previously evoked[25,45] can be here avoided since we operate in anhydrous conditions. The contribution of the deprotonation step towards the anodic process observed for **PT** is confirmed regarding the electrochemical behavior of *N*-alkyled phenothiazines (**1-3**) (Figure 2). CV in these cases displayed two successive one-electron fast and quasi-reversible oxidation processes. Substitution on the nitrogen atom by an alkyl group leads to an increase of the two $E_{1/2}$ values compared to those of **PT** (Table 1). As it was evoked by Rawashdeh *et al.*[48], when the phenothiazinyl heterocycle adopts a planar conformation, alkylation (*e.g.* methylation) contributes to the distortion of the heterocycle in agreement with the more exergonic electron transfer. Increasing the chain length from methyl up to ethyl, the $E_{1/2}$ values decreased down to 3.97 V/Li/Li$^+$ for **2** whereas for longer carbon chains this value remains almost unchanged in a good accordance with the fact that electron donor effect is poorly modified by the length of the linear alkyl substituent.

Concerning (**4**), *N*-substitution by an ester group leads to a substantial oxidation augmentation (Figure 2) with slower redox processes (*e.g.* ΔE_p > 140 mV) located at $E^1_{1/2}$ = 4.59 and $E^2_{1/2}$ = 4.82 V /Li/Li$^+$. Given the too high oxidizing character of the radical cation of this phenothiazine derivative, such functionalization cannot be further investigated, the electrolyte being not enough stable in this potential range. Nonetheless, surprisingly, the positive shift towards the $E_{1/2}$ values appears to be more pronounced as expected for a substitution by a carbonyl function. Indeed, such chemical modification involving ferrocene leads only to 0.2-0.3 V increase[49,50]. This means that carbonyl function presumably through its withdrawing effect and/or its conjugation with the heterocycle deeply modifies the electrochemical response of the phenothiazine.

3.2.2. *Ab initio* calculations

Our findings (**Figure 3**) highlight that the oxidization process leads to a radical change in the geometry of **1** and **PT** molecules: after optimization of geometry, a bent conformation is found in the neutral state and a planar geometry in the oxidized one. To the opposite, the geometry of **2** and **3** shares the same conformation at both their neutral and oxidized forms and

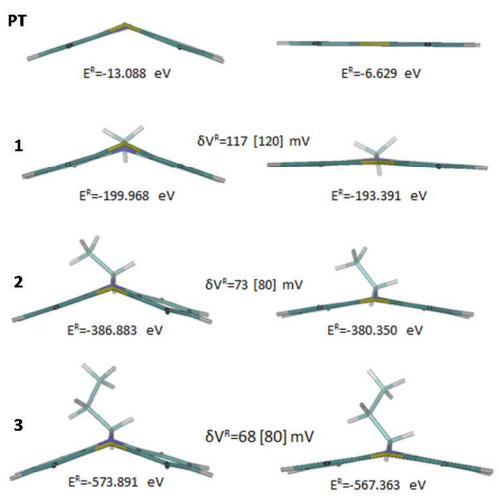

Fig. 3 Calculated geometry, total energy and gain in the voltage, δV^R, of our studied molecules. The voltage of **PT** is chosen as the reference for the gain in the voltage of **1**, **2** and **3**

remains bent, although the oxidized form displays larger butterfly angles (they tend to recover a more planar geometry as seen in Figure 3). The conserving of the bent geometry for the *N*-derivatives of **PT** after oxidization is in fine agreement with phenomenon recently encountered by Narayana et al.[22] for R=C(CH_3)$_3$. Our results however differ from their work as regards to the methyl derivatives (molecule **2**) since we obtain a more clearly bent geometry. This state was obtained by switching off the symmetry in our calculations, allowing all the degrees of freedom necessary to obtain the ground state. To firmly establish this result, we have used the code vasp[51] to compute the total energy of this bent geometry and compared it to that of the planar one. We probed the energy difference using different exchange-correlation functionals, namely LDA, PBE and B3LYP as implemented in vasp. For each of them, we obtained that the energy difference is similar to that obtained in the present calculation and therefore we can confirm that the bent geometry is more stable than the planar one [unpublished results]. As we shall see in the followings through a careful analysis of the electronic structure, this molecule develop an asymmetrical molecular orbital which is found determinant into the oxidization process of the derivatives involving the longest alkyl chain (**2** and **3**). The drastic change of conformation of **1** has a heavy cost in energy and leads to the highest difference of energy between the oxidized and neutral forms (and consequently to the highest $E_{1/2}$): the relaxation energy coming in addition to the pure oxidation energy at fixed geometry is larger than for the others molecules.

For both **2** and **3**, the difference in energy between the oxidized and neutral form is rather due to the electron retrieval at similar geometry so that the $E_{1/2}$ value is found lower than in the case of **1**. Figure 3 also displays the calculated total energies of the three molecules considered in their neutral and oxidized states, as well as the differences of these energies, needed to calculate the gain in the oxidization standard potential of **1**, **2**, **3** with respect to the one of **PT**, through the **Equation 2**:

$$\delta V_R = \frac{E^{R+} - E^R}{\mathcal{F}} - V_H \qquad (2)$$

where E^R is the total energy of the neutral **1**,**2** and **3**, E^{R+} the total energy of the corresponding oxidized molecule, and $\mathcal{F}$ is the Faraday constant (equals unity with energies in eV) and $V_H = (E^{PT+} - E^{PT})/\mathcal{F}$. This formulation relying on the difference of voltages allows us measuring the gain in the voltage of **PT** and its derivatives without delicate assumptions on the modeling of the Li/Li^+ couple as well as the work potential of the electrons since their contribution vanishes when having the difference. These energies correspond to the stable geometry of the molecules at 0 K whose details are provided in Figure 3. Thus, at low temperature, the calculated values of δV_R are in excellent agreement with the experiments, with a gain of 117 mV as the N-H function is replaced by a N-CH_3 bond and lower values (73 and 68 mV) as replaced by N-CH_2CH_3 and N-$(CH_2)_2CH_3$ respectively. Let's now turn to the analysis of the HOMO and the first electronic levels of our molecules. **Figure 4.a** displays the energy diagram of both neutral and oxidized **PT**, **1**, **2** and **3** molecules. As oxidized, one electron is retrieved from the HOMO without major shift on the four first molecular energy levels. These latter mainly concern the π orbitals of N, S and the C of the cycles (**Figure 4.b**). The same behavior (and the same magnitude for the shifts in energy) is observed for the other molecules so that these first molecular levels cannot account for the differences in energy observed between the four molecules and, consequently for differences in the voltage. If the oxidation process affects the character of orbitals #3 and #4, this change is found independent on the alkyl fragment but also on the geometry as shown by the comparison of the orbitals of the planar oxidized **PT** and bent oxidized molecule **3** (Figure 4.b). At this stage, we understand that the origin of the observed trend has to be found deeper in the molecular diagrams, where molecular states involve orbitals of the **R** fragment and N-**R** bonds.

In the followings, the HOMO is set to zero and fixes our absolute reference to allow a direct comparison of the energy levels of the neutral and oxidized molecules as well as their character. Let's now turn to a deeper examination of the MO (**Figures 5**, **6** and **7**). In order to spot the influence of the alkyl moiety on the energy levels of the molecules, we introduce the following color code in Figures 5, 6 and 7: i) yellow MO are delocalized states over the cycles, involving also the S orbitals, ii) green MO are delocalized states over external cycles of PN only, iii) violet MO involves both delocalized states over the external cycles of **PT** and states spreading throughout the alkyl moiety, iv) grey MO only interests states localized or spreading over the alkyl fragment, v) blue ones involve states over both N and alkyl chains.

To start with, let's focus on the neutral molecules (left panel of Figure 5 to 7). They are all bent and undergo a similar electronic structure with a quite similar sequence of MO. The discrepancies are only due to the intercalation of states coming from the new degrees of freedom introduced by the nature and increasing length of the alkyl fragment: while a series of symmetric conjugated states is obtained over both external cycles of **PT** (8, 9 and 10) for **1** (green block), these states are replaced by asymmetric states involving one cycle of **PT** over two and the alkyl chain (violet block) in the case of **2** and **3**: things appear as if conjugation be deviated towards the alkyl fragment when this latter is long enough, namely from the ethyl chain.

As regards to the oxidized states, two different behaviors are

Cite this: DOI: 10.1039/c0xx00000x

www.rsc.org/xxxxxx

ARTICLE TYPE

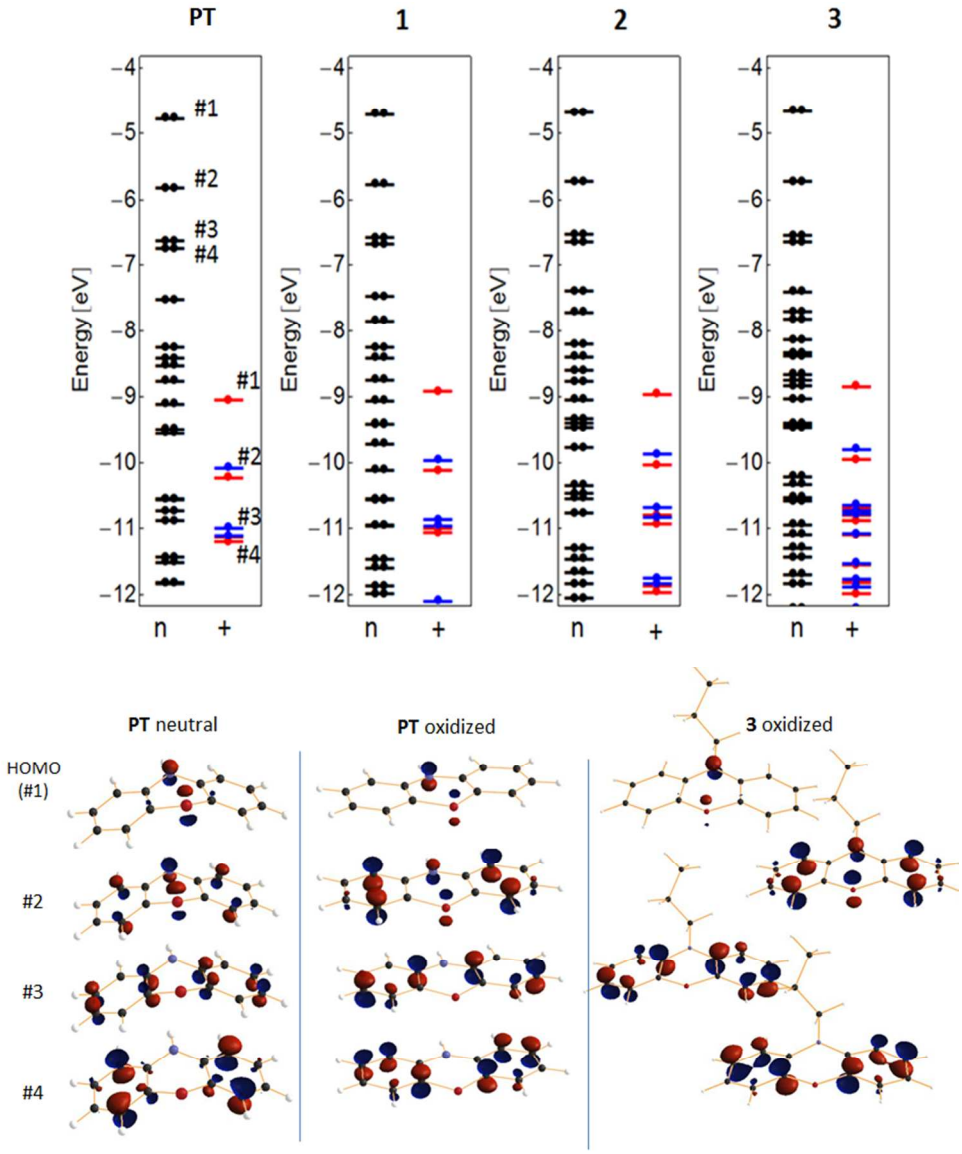

Fig. 4 a) Comparison between the electronic structure of PT, 1, 2 and 3 and b) the first four molecular orbitals of the molecules. They are found independent on the alkyl moiety.

obtained as expected. At first, let's turn to **1** (Figure 5). We notice a lowering of energy of the most delocalized states due to the newly adopted planar geometry (yellow blocks). But the main signature of the planar geometry case is found in the forming of an unfavorable energy level built upon MO of the external cycles (originally, the 8, 9 and 10 MO of neutral **1**) and localized orbitals of both S and N This MO is determinant and explains the highest gain in voltage among the *N*-derivatives with respect to **PT**. We will add further commentaries about this orbital after the examination of the electronic structure of **2** and **3**.

Regarding **2** and **3** (Figures 6 and 7), the same lowering of the energy levels is noted for the most conjugated states. This is consistent with our analysis of geometry which was displaying a widening of the butterfly angle of the molecules as oxidized (Figure 3). However, the existence of the asymmetric orbitals induced by the ethyl and propyl moieties leads to a rather different scenario for the fifth MO (and below) than the one encountered for the methyl fragment. For **2**, both these orbitals split twice as oxidized to be re-formed into a pure MO spreading over the alkyl chain in one hand and a conjugated MO over the cycles of **PT** in the other hand. The same behavior is observed for **3**. Here, things appear as if the electron retrieval inherent to the oxidation process interrupts the hybridization between the atoms of the alkyl fragment and the atoms of the external ring of **PT**

Cite this: DOI: 10.1039/c0xx00000x

www.rsc.org/xxxxxx

ARTICLE TYPE

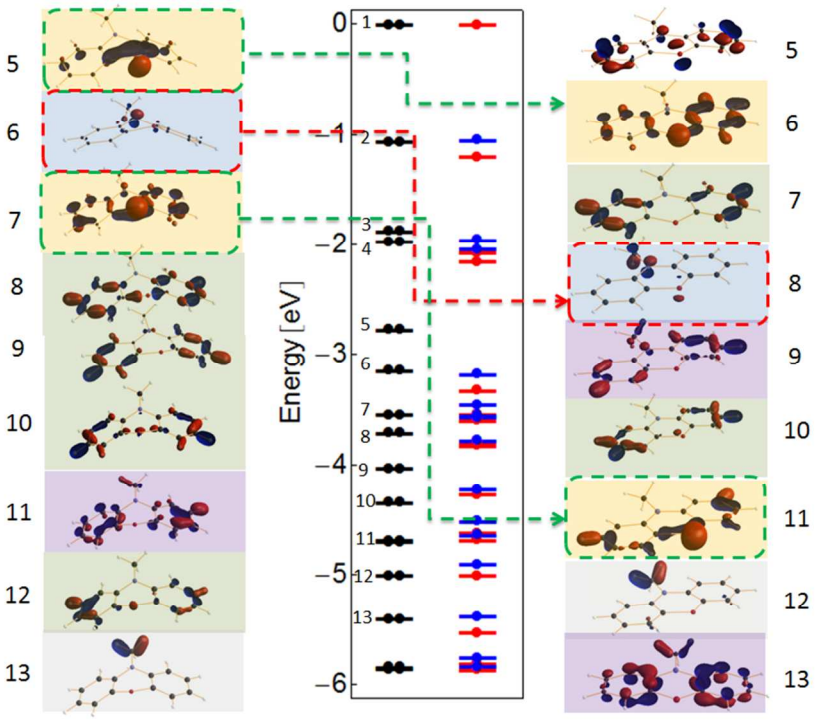

Fig. 5 Electronic structure of **1** and the first molecular orbitals found to be dependent on the alkyl moiety for the neutral molecule (left panel) and the oxidized molecule (right panel). The electronic structure of both neutral and oxidized molecule were shifted so that their respective HOMO (#1) be 0 to allow direct comparison.

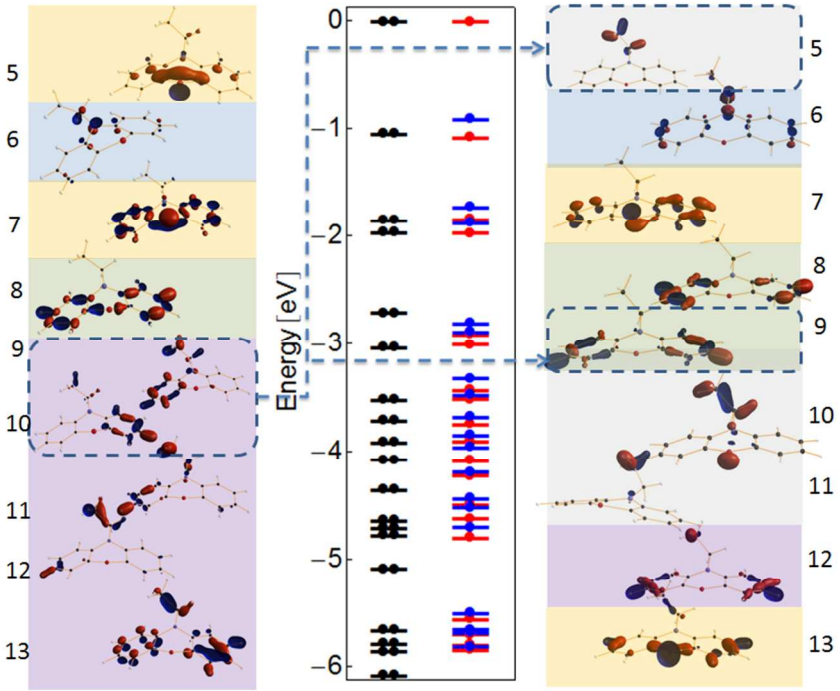

Fig. 6 Idem **Fig. 5** but for molecule **2**.

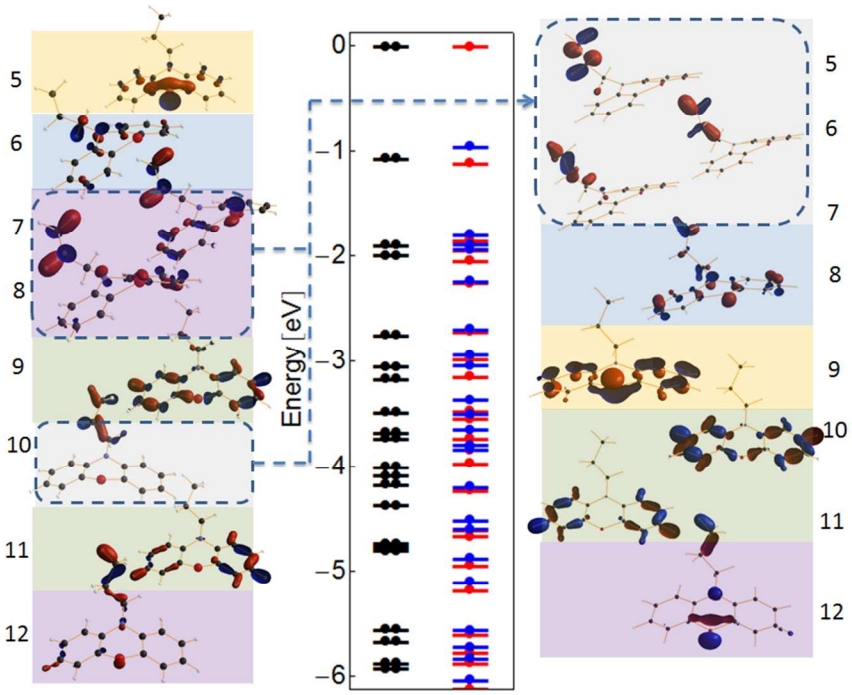

Fig. 7 Idem **Fig. 5** but for molecule **3**

that we previously noticed in the neutral molecule. Thus, these orbitals appear to be the key-parameter allowing molecule **2** and **3** to keep their bent geometry. The shortest methyl fragment do not allow to develop such orbitals and leads to the forming of the so-obtained orbital 5 described before, corresponding to a more unfavorable state (oxidized **1** is less stable than oxidized **2** and **3** with respect to their respective neutral form) but also to a radical change in conformation to adapt the electron departure. The inability of the methyl fragment to develop such a molecular orbital has to be found in the inability of the symmetric $-CH_3$ fragment to break the symmetry as ethyl and propyl fragments do.

3.2.3. Phenothiazine derivative selection

Knowing that the influence of conformational change has a deep influence on the electron transfer kinetics (k^0), authors outlined that the lower conformational change during the oxidation step occurs, the easier the electron should be transferred and the higher k^0 value should be observed. Nishide *et al.*[52] suggested that cathode materials have to exhibit high k^0 value in view to reach high C rate during the charge/discharge processes.

Using Nicholson *et al.* formula (**Equation 3**)[53,54], k^0 values (Table 1) have been determined.

$$k^0 = \frac{\psi\sqrt{\pi . a . D_O}}{\gamma^{\alpha}}; \psi = x_0 . \left(\frac{A_1}{\Delta E_p - A_2} - 1\right)^{\frac{1}{p}}; \gamma = \left(\frac{D_O}{D_R}\right)^{\frac{1}{2}}; a = \frac{nF}{RT} . v \qquad (3)$$

Diffusion coefficients of the oxidant D_O and reductant D_R are estimated to be of the same order of value (determined by Levich equation), n = 1, F = 96485 C.mol^{-1}, R = 8.314 J.mol^{-1}.K^{-1}, T = 298 K, v = scan rate (V.s^{-1}), A_1 = 373.36 mV, A_2 = 59.55 mV, x_0 = 0.0688 and p = 0.9938.

It has been established that the functionalization of the cyclic nitrogen by an alkyl group leads to a significant k^0 increase. The lower k^0 value is observed for **PT** whereas increasing the length of the alkyl chain k^0 slightly increase to reach a close value for **2** and **3** (~5.8.10^{-3} cm s^{-1}) in good correlation with *ab initio* calculations and the lower conformational changes along the electron transfer as determined for alkyled phenothiazines. One can outline that k^0 value are in the same order of magnitude than that of ferrocene (*i.e.* 10^{-2} cm s^{-1}) in CH_3CN electrolyte, confirming the fast electron transfer[55].

Taking into account the higher k^0 value, the two reversible redox processes (Figure 2), phenothiazine bearing propyl chain (**3**) has been further selected in view to elaborate **Poly3**. Concerning the influence of the cyclic's chemical modifications, this has been examined for the dibromo derivative (**5**), $E_{1/2}$ values for the two one electron reversible oxidation steps are increased (4.13 V/Li/Li$^+$ and 4.70 V/Li/Li$^+$) with good agreement with the electron withdrawing effect of substituents. However, due to the too high mass contribution of the two bromines, such monomer has not been further investigated in polymeric context.

3.3. Electrochemistry of Poly3

3.3.1 Cavity MicroElectrode (CME)

Prior to battery investigation, we have firstly studied **Poly3a** using a cavity microelectrode (CME) system which is particularly adapted for insoluble and poorly electron conducting material. Typically, a small amount (*e.g.* 1 µg) of the polymer powder was manually loaded into the CME which was then immersed into the CH_3CN + TBAP 0.1 M medium.

Cyclic voltammetry (2 cycles) between 3.1 and 4.2 V /Li/Li$^+$ has been then carried out at different scan rates (100 to 10 mV.s^{-1}). Only the 2nd cycles are represented (**Figure 8.a$_1$**) for the sake of clarity. At 100 mV.s^{-1}, the stabilization of the voltammogram was achieved for the 2nd cycle (could be due to a slight solubilization of low-chains oligomers during the first cycle), showing the fast equilibrium that takes place between the electrolyte and the **Poly3a** powder placed in the cavity[56].

This broad electrochemical signature is characteristic of

Cite this: DOI: 10.1039/c0xx00000x

www.rsc.org/xxxxxx

ARTICLE TYPE

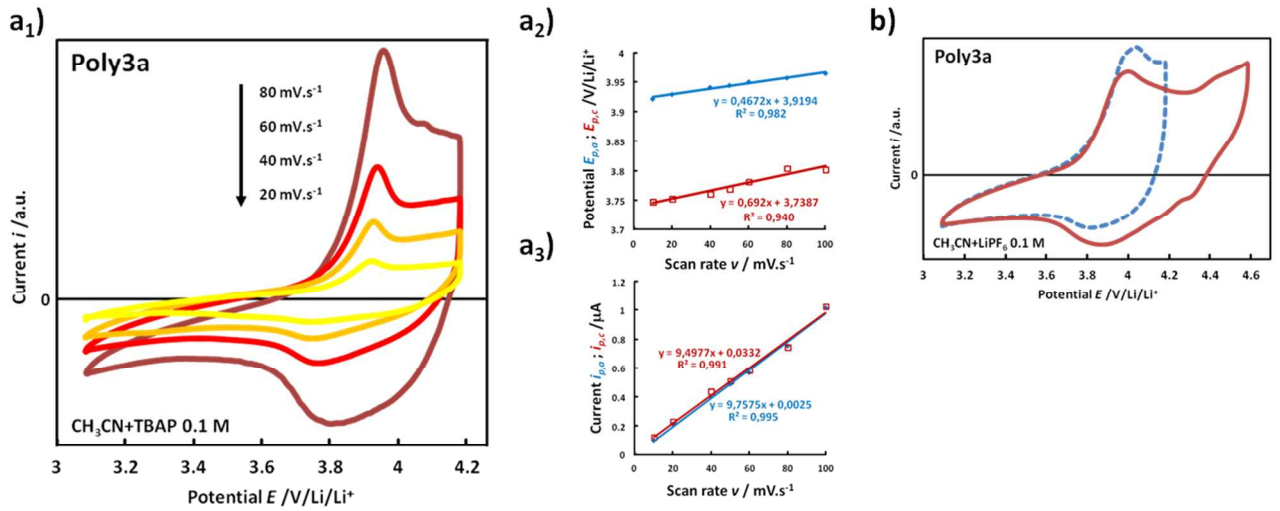

Fig. 8 Poly3a analysis in CME a) in CH_3CN + TBAP 0.1 M medium at different scan rates presenting a_1) cyclic voltammograms, a_2) variations of anodic and cathodic peak potentials ($E_{p,a}$; $E_{p,c}$) *vs* the scan rate, a_3) variations of anodic and cathodic peak currents ($i_{p,a}$; $i_{p,c}$) *vs* the scan rate $v^{1/2}$, a_4) variations of $i_{p,a}$ and $i_{p,c}$ *vs* the scan rate *v* b) in CH_3CN + $LiPF_6$ 0.1 M medium at 80 $mV.s^{-1}$ on a range of (blue dashed line) 3.1-4.2 V and of (red full line) 3.1-4.6 V

conjugated phenothiazine oligomers that can favor the delocalization of the radical cations formed during the oxidation process[39]. This intramolecular electronic coupling causes the first oxidation to affect the upcoming ones. As a result, on one hand, the first electron of the polymeric chains is more easily oxidized than in the monomer case, thus the $E_{1/2}$ of the **Poly3a** calculated on the well-defined pre-oxidation peak and on the reduction peak at different scan rates is found to be of 3.86±0.03 V/Li/Li^+ (ΔE_p = 165±15 mV) which is 110 mV lower than the $E_{1/2}$ of **3** in good agreements with the effect of the conjugation observed by M. Sailer *et al.* on *N*-hexylphenothiazine oligomers[39]. On the other hand, further oxidation processes become more difficult, causing the broadening of the electrochemical oxidation signature. A larger broadening is also observed during the reduction process without a well-defined reduction peak. The same type of signature was observed in the case of *N*-hexylphenothiazine oligomers[39] in solution. For each scan rate, the electrochemical signature was maintained, permitting an evaluation of its redox process properties. Thus, between 10 and 100 $mV.s^{-1}$: the ratio of $i_{p,a}/i_{p,c}$ was close to one, the peak potentials were quite independent of the scan rate (**Figure 8.a$_2$**) with a low diminution of its values at lower scan rate and the peak currents were linearly dependant of the scan rate (**Figure 8.a3**) showing that the material underwent fast electron transfer[56].

The CME with the same loading of **Poly3a** was also studied in CH_3CN + $LiPF_6$ 0.1 M medium in order to check the influence of a lithium salt on the **Poly3a** electrochemical signature. The same electrochemical analysis (**Figure 8.b**) was carried out (same potential sweep range and scan rates) and the same conclusions were made: the first redox system centered on 3.90±0.05 V/Li/Li^+ (ΔE_p = 221±12 mV) was estimated to be fast. This very close $E_{1/2}$ (3.86 V /Li/Li^+ in TBAP-based electrolyte) according to the salt of the electrolyte confirmed, as expected, the versatility of the organic redox materials. While increasing the potential range from 3.1 to 4.6 V /Li/Li^+, a second peak couple was witnessed. Thanks to its sustainability on the electrode, this redox system was investigated at different scan rates (10-100 $mV.s^{-1}$), and was centered on 4.37±0.01 V/Li/Li^+ (ΔE_p = 124±11 mV) and could be attributed to the second one-electron redox process.

3.3.2. Swagelok lithium cell

Preliminary **Poly3a**/EC-DMC+$LiPF_6$-1M/Li Swagelok® cell tests were investigated between 3 and 4 V at a C/10 and D/10 charge and discharge rates (11.2 mA per grams of active material). This potential sweep range was chosen to avoid degradation of the electrolyte. The specific discharge capacity and the coulombic yield of the first 10 cycles were plotted in the **Figure 9.a**, a specific discharge capacity of 80 $mAh.g^{-1}$ of **Poly3a** was supplied which is lower than its theoretical one (112 $mAh.g^{-1}$). This discrepancy may be attributed i) to the presence of side products detected by elemental analysis, ii) to a non-optimized formulation preventing a good electronic connection between active material and carbon, iii) to the cycling that is limited to 4 V that may prevent the first one-electron redox system to be fully harvested. The coulombic yield achieved high values after a few cycles (> 99%). The lower values of coulombic yield could be explained by the solubilization of some polymeric material bearing short chains during the oxidation process of the first cycles.

The charge and discharge curves of the 5th cycle can be seen in the inset of the Figure 9.a, the absence of a plateau and this progressive oxidation and reduction shape is coherent with an electronic conjugated polymer effect previously observed in *e.g.* polyaniline[57] or polycarbazole[58]. A half-wave global potential of

Cite this: DOI: 10.1039/c0xx00000x

www.rsc.org/xxxxxx

ARTICLE TYPE

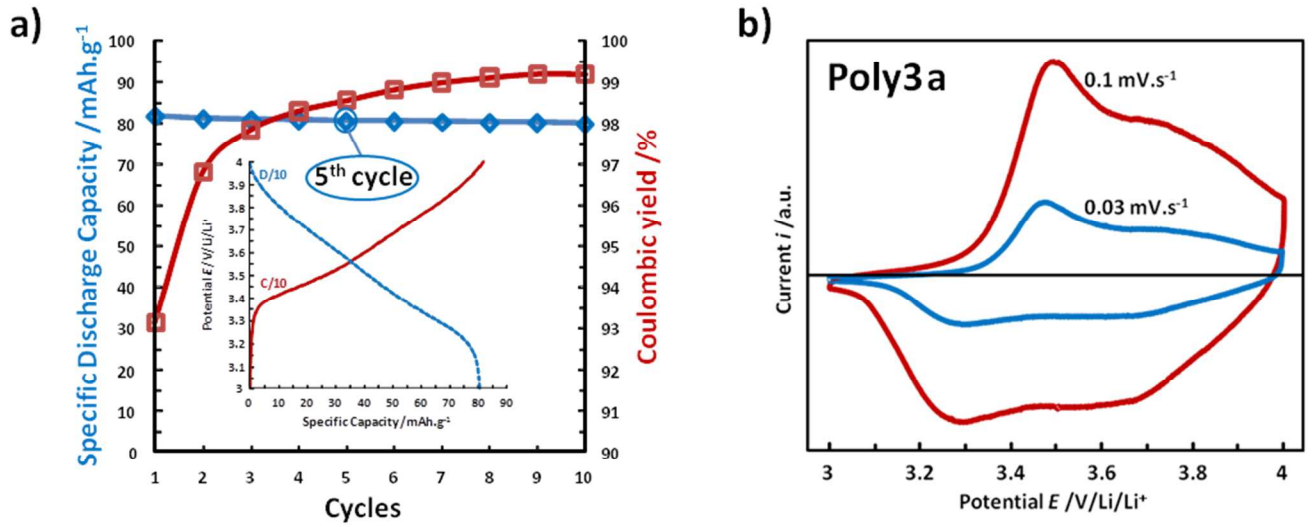

Fig. 9 Poly3a/EC-DMC+$LiPF_6$-1M/Li Swagelok® cell a) first galvanostatic cycles at C/10 and D/10 rate with an inset of the 5th cycle b) cyclic voltammograms recorded after 50 galvanostatic cycles at different scan rates

~3.6 V with 100 mV of polarization was estimated. Moreover, CV of this cell (**Figure 9.b**) in the same potential range exhibits a similar electrochemical signature to the one obtained in CME with a more defined reduction peak and a larger conjugation effect. Pre-peaks half-wave potential was situated at 3.39 V (ΔE_p 199 mV) which is ~500 mV lower compared to the one obtained by CV in CME in CH_3CN + $LiPF_6$ 0.1 M medium. This significant difference might be due to the combination of different parameters as i) the solvent effect, ii) the 10 fold higher electrolyte salt concentration, iii) the optimized electronic conductive pathways permitted by the carbon and the VGCF additives that upgrade the conjugation effect lowering the first oxidation potential. The modification of redox potential by changing the electrolyte was observed by K. A. Narayana *et al.*[22] who used similar phenothiazine alkyle derivatives as redox shuttle additives for lithium cells. Indeed, close redox potential of **2** in weak concentrated electrolyte can be measured in this study (0.30 V[33] /Fc/Fc^+ in CH_3CN+TBAP 10^{-1}M) and the one of Narayama (0.26 V /Fc/Fc^+ in CH_2Cl_2+$TBAPF_6$ 10^{-1}M) knowing that Fc/Fc^+ redox potential is 13 mV[59] lower in CH_3CN than in CH_2Cl_2(with TBAP 10^{-1}M salt). Nevertheless, a $E_{1/2}$ of **2** of 3.51 V/ Li/Li^+ in EC-EMC + $LiPF_6$ 1.2 M medium was measured which is 460 mV lower than weak concentrated medium. Given this result, we could say it is the effect of the change of electrolyte that may assist the oxidation process of phenothiazine moieties.

The capacity hold towards cycling (0.25 % capacity loss between the 9th and the 10th cycle) shows that the polymer does not undergo some degradation and/or solubilization during the successive cycles, thus confirming both the stability and the insolubility of the studied material.

These results are very promising and can be largely optimized by changing the formulation and the coating process. Using an electrolyte that is compatible with lithium and high potentials (e.g. 4.5 V /Li/Li^+) would permit the exploitation of the 2nd redox system of the **Poly3a** and could double its discharge capacity.

Conclusions

Several substituted phenothiazines have been synthesized and electrochemically analyzed in relation with *ab initio* calculations in order to select phenothiazinyl core having the best $E_{1/2}$ value and the faster kinetic rate of electron transfer. This preliminary study allowed investigating the corresponding polymer for organic batteries. Polymerization using Suzuki reaction has led to material that behave similarly towards oxidation comparing to the starting monomer, attesting that polymerization does not modify the redox process quality of the monomer unit. Preliminary cell tests involving the polyphenothiazine selected showed a promising specific discharge capacity (80 $mAh.g^{-1}$) with a great cyclability potential. When electrolyte will be stable at high potentials, we should be able to reach the second oxidation process of this material that would set the specific discharge capacity to double (*i.e.* 160 $mAh.g^{-1}$).

Acknowledgements

Solvay S.A (Daniel Gloesener, Bruxelles) and the ANRT for the CIFRE fellowship. Pierre-Yves Chavant from SERCO-DCM (Département de Chimie Moléculaire) for the microwave device and his expertise. O. Lebacq and A. Pasturel acknowledge the CINES (Centre Informatique National de l'Enseignement Supérieur) and CIMENT (Calcul Intensif / Modélisation /

Expérimentation Numérique et Technologique) for computational resources.

Notes and references

[a] LEPMI, UMR 5279 CNRS-Grenoble INP-UdS-UJF, 1130 rue de la Piscine, BP 75, 38402 Saint Martin d'Hères Cedex, France
[*] Tel: +3373429963; e-mail: thibault.godetbar@lepmi.grenoble-inp.fr
[b] DCM, UMR 5250 CNRS-UJF, Univ. Grenoble Alpes, BP 53, 38041 Grenoble Cedex 9, France
[c] SIMAP, UMR 5266 CNRS-Grenoble INP-UJF, Univ. Grenoble Alpes, BP 75, 38402 Saint Martin d'Hères, France

1 M. S. Whittingham, *Chemical reviews*, 2014.
2 K. Zaghib, A. Guerfi, P. Hovington, A. Vijh, M. Trudeau, A. Mauger, J. Goodenough and C. Julien, *Journal of Power Sources*, 2013, **232**, 357-369.
3 A. K. Padhi, K. Nanjundaswamy and J. Goodenough, *Journal of The Electrochemical Society*, 1997, **144**, 1188-1194.
4 J. Chen, *Materials*, 2013, **6**, 156-183.
5 D. V. Chernyshov, S. A. Krachkovskiy, A. V. Kapylou, I. A. Bolshakov, W. C. Shin and M. Ue, *Journal of The Electrochemical Society*, 2014, **161**, A633-A642.
6 J. Xia, J. Harlow, R. Petibon, J. Burns, L. Chen and J. Dahn, *Journal of The Electrochemical Society*, 2014, **161**, A547-A553.
7 B. C. Melot and J.-M. Tarascon, *Accounts of chemical research*, 2013, **46**, 1226-1238.
8 M. Zhou, Y. Xiong, Y. Cao, X. Ai and H. Yang, *Journal of Polymer Science Part B: Polymer Physics*, 2013, **51**, 114-118.
9 H. Chen, M. Armand, M. Courty, M. Jiang, C. P. Grey, F. Dolhem, J.-M. Tarascon and P. Poizot, *Journal of the American Chemical Society*, 2009, **131**, 8984-8988.
10 M. Yao, H. Senoh, S.-I. Yamazaki, Z. Siroma, T. Sakai and K. Yasuda, *Journal of Power Sources*, 2010, **195**, 8336-8340.
11 O. Y. Posudievsky, O. A. Kozarenko, V. S. Dyadyun, V. G. Koshechko and V. D. Pokhodenko, *Synthetic Metals*, 2012, **162**, 2206-2211.
12 Z. Song, H. Zhan and Y. Zhou, *Chem. Commun.*, 2009, 448-450.
13 J.-K. Kim, J.-H. Ahn, G. Cheruvally, G. S. Chauhan, J.-W. Choi, D.-S. Kim, H.-J. Ahn, S. H. Lee and C. E. Song, *Metals and Materials International*, 2009, **15**, 77-82.
14 H. Nishide, S. Iwasa, Y.-J. Pu, T. Suga, K. Nakahara and M. Satoh, *Electrochimica Acta*, 2004, **50**, 827-831.
15 K. Oyaizu, T. Suga, K. Yoshimura and H. Nishide, *Macromolecules*, 2008, **41**, 6646-6652.
16 H. M. Gordon, *Australian veterinary journal*, 1945, **21**, 90-95.
17 S. G. Dastidar, J. Jairaj, M. Mookerjee and A. N. Chakrabarty, *Acta Microbiologica et Immunologica Hungarica*, 1997, **44**, 241-247.
18 S. C. Goldberg, G. L. Klerman and J. O. Cole, *The British Journal of Psychiatry*, 1965, **111**, 120-133.
19 G. Wampler, *Drugs*, 1983, **25**, 35-51.
20 C. Buhrmester, L. Moshurchak, R. L. Wang and J. R. Dahn, *Journal of The Electrochemical Society*, 2006, **153**, A288-A294.
21 M. D. Casselman, A. P. Kaur, K. A. Narayana, C. F. Elliott, C. Risko and S. A. Odom, *Physical Chemistry Chemical Physics*, 2015.
22 K. A. Narayana, M. D. Casselman, C. F. Elliott, S. Ergun, S. R. Parkin, C. Risko and S. A. Odom, *ChemPhysChem*, 2014.
23 D. Gligor, Y. Dilgin, I. C. Popescu and L. Gorton, *Electrochimica Acta*, 2009, **54**, 3124-3128.
24 K. Nishio, M. Fujimoto, N. Yoshinaga, N. Furukawa, O. Ando, H. Ono and T. Suzuki, *Journal of power sources*, 1991, **34**, 153-160.
25 J.-P. Billon, *Annales de Chimie France*, 1962, **7**, 183-206.
26 L. Michaelis, S. Granick and M. P. Schubert, *Journal of the American Chemical Society*, 1941, **63**, 351-355.
27 N. Urasaki, S. Yoshida, T. Ogawa, K. Kozawa and T. Uchida, *Bulletin of the Chemical Society of Japan*, 1994, **67**, 2024-2030.
28 J. Choi, B. Lee and J. H. Kim, *Synthetic Metals*, 2009, **159**, 1922-1927.
29 D.-H. Yun, H.-S. Yoo, S.-W. Heo, H.-J. Song, D.-K. Moon, J.-W. Woo and Y.-S. Park, *Journal of Industrial and Engineering Chemistry*, 2013, **19**, 421-426.
30 M. Sailer, A. W. Franz and T. J. J. Müller, *Chemistry-A European Journal*, 2008, **14**, 2602-2614.
31 Y. S. Han, S. D. Kim, L. S. Park, D. U. Kim and Y. Kwon, *Journal of Polymer Science Part A: Polymer Chemistry*, 2003, **41**, 2502-2511.
32 S. Darvesh, K. V. Darvesh, R. S. McDonald, D. Mataija, R. Walsh, S. Mothana, O. Lockridge and E. Martin, *Journal of medicinal chemistry*, 2008, **51**, 4200-4212.
33 V. V. Pavlishchuk and A. W. Addison, *Inorganica Chimica Acta*, 2000, **298**, 97-102.
34 L. Genovese, A. Neelov, S. Goedecker, T. Deutsch, S. A. Ghasemi, A. Willand, D. Caliste, O. Zilberberg, M. Rayson, A. Bergman and R. Schneider, *The Journal of chemical physics*, 2008, **129**, 014109.
35 M. Filatov and S. Shaik, *The Journal of Physical Chemistry A*, 2000, **104**, 6628-6636.
36 R. Stowasser and R. Hoffmann, *Journal of the American Chemical Society*, 1999, **121**, 3414-3420.
37 T. Kar, J. G. Ángyán and A. Sannigrahi, *The Journal of Physical Chemistry A*, 2000, **104**, 9953-9963.
38 S. Goedecker, M. Teter and J. Hutter, *Physical Review B*, 1996, **54**, 1703.
39 M. Sailer, A. W. Franz and T. J. Müller, *Chemistry-A European Journal*, 2008, **14**, 2602-2614.
40 M. Bolboaca, T. Iliescu, C. Paizs, F. Irimie and W. Kiefer, *The Journal of Physical Chemistry A*, 2003, **107**, 1811-1818.
41 J. B. Lambert, H. F. Shurvell, D. A. Lightner and R. G. Cooks, 1987.
42 C. Bodea and I. Silberg, *Advances in heterocyclic chemistry*, 1968, **9**, 321-460.
43 P. H. Sackett, J. S. Mayausky, T. Smith, S. Kalus and R. L. McCreery, *Journal of Medicinal Chemistry*, 1981, **24**, 1342-1347.
44 D. Aurbach, Y. Talyosef, B. Markovsky, E. Markevich, E. Zinigrad, L. Asraf, J. S. Gnanaraj and H.-J. Kim, *Electrochimica Acta*, 2004, **50**, 247-254.
45 J. Karpinska, B. Starczewska and H. Puzanowska-Tarasiewicz, *Analytical sciences*, 1996, **12**, 161.
46 N. Zimová-Šulcová, I. Němec, K. Waisser and H. L. Kies, *Microchemical journal*, 1985, **32**, 33-43.
47 A. J. Bard and L. R. Faulkner, *Electrochemical Methods, 2nd ed.; Wiley: New York*, 2001.
48 A. M. M. Rawashdeh, *Abhath Al-Yarmouk, Basic Sciences and Engineering*, 2005, **14**, 195-208.
49 J. R. Aranzaes, M.-C. Daniel and D. Astruc, *Canadian journal of chemistry*, 2006, **84**, 288-299.

50 C. Xue, Z. Chen, Y. Wen, F.-T. Luo, J. Chen and H. Liu, *Langmuir*, 2005, **21**, 7860-7865.

51 G. Kresse and D. Joubert, *Physical Review B*, 1999, **59**, 1758.

52 H. Nishide, K. Koshika and K. Oyaizu, *Pure and Applied Chemistry*, 2009, **81**, 1961-1970.

53 D. Dragu, M. Buda and T. Vişan, *UPB Scientific Bulletin, Series B*, 2009, **71**, 77-90.

54 R. S. Nicholson, *Analytical Chemistry*, 1965, **37**, 1351-1355.

55 N. L. Ritzert, J. Rodríguez-López, C. Tan and H. c. D. Abruña, *Langmuir*, 2013, **29**, 1683-1694.

56 V. Vivier, C. Cachet-Vivier, D. Michel, J.-Y. Nedelec and L. Yu, *Synthetic Metals*, 2002, **126**, 253-262.

57 K. S. Ryu, K. M. Kim, Y.-S. Hong, Y. J. Park and S. H. Chang, *BULLETIN-KOREAN CHEMICAL SOCIETY*, 2002, **23**, 1144-1148.

58 M. Yao, H. Senoh, T. Sakai and T. Kiyobayashi, *Journal of Power Sources*, 2012, **202**, 364-368.

59 I. Noviandri, K. N. Brown, D. S. Fleming, P. T. Gulyas, P. A. Lay, A. F. Masters and L. Phillips, *The Journal of Physical Chemistry B*, 1999, **103**, 6713-6722.